An Improved Solution for Integrated Array Optics in Quasi-Optical mm and Submm Receivers: the Hybrid Antenna

Thomas H. Büttgenbach, *Student Member, IEEE*

Abstract—**The hybrid antenna discussed here is defined as a dielectric lens-antenna as a special case of an extended hemispherical dielectric lens that is operated in the diffraction limited regime. It is a modified version of the planar antenna on a lens scheme developed by Rutledge. The dielectric lens-antenna is fed by a planar-structure antenna, which is mounted on the flat side of the dielectric lens-antenna using it as a substrate, and the combination is termed a hybrid antenna. Beam pattern and aperture efficiency measurements were made at millimeter and submillimeter wavelengths as a function of extension of the hemispherical lens and different lens sizes. An optimum extension distance is found experimentally and numerically for which excellent beam patterns and simultaneously high aperture efficiencies can be achieved. At 115 GHz the aperture efficiency was measured to be $(76 \pm 6)\%$ for a diffraction limited beam with sidelobes below -17 dB. Results of a single hybrid antenna with an integrated Superconductor-Insulator-Superconductor (SIS) detector and a broad-band matching structure at submillimeter wavelengths are presented. The hybrid antenna is diffraction limited, space efficient in an array due to its high aperture efficiency, and is easily mass produced, thus being well suited for focal plane heterodyne receiver arrays.**

I. Introduction

REMOTE SENSING in the millimeter and submillimeter wavelength bands requires sensitive detectors and well defined beam properties of the antennas used to collect the radiation. In this paper an antenna system that provides such a well defined beam pattern will be described. The issue of sensitivity of the detector will only be addressed in so far as it depends on the coupling of the detector to the radiation field through the detector's receiving antenna. A specific application of remote sensing in the millimeter and submillimeter wavelength bands—heterodyne spectroscopy in radio astronomy—will be emphasized since the instrumentation developed was aimed at this application. Of course, the same basic principles apply to most other applications for coherent detection of radiation.

Radio astronomy uses large aperture antennas to focus the incoming radiation onto a second, much smaller antenna, which feeds the received power to a detector, either directly or via an impedance matching circuit (see Fig. 1). The properties of the second antenna, i.e. the receiver antenna, and its coupling to the primary antenna, i.e. the radio telescope, will be discussed. Traditionally, the receiver antennas used are waveguide horn antennas that transform the free space TEM mode coming from the telescope into a waveguide mode where the radiation is detected in a nonlinear element suspended across the waveguide (see for example [1]). However, in the submillimeter band these waveguide structures become expensive and difficult to manufacture due to their small size. Since the skin depth gets smaller at shorter wavelengths the surface roughness of the walls of the waveguide structures becomes increasingly more important and thus losses will increase. Waveguide horn antennas with the associated metal waveguide structures are also not well suited for array applications since they are traditionally manufactured by machining the individual waveguide components. However, modern approaches use semiconductor lithographic techniques to manufacture parts of the horn antennas [2]–[5].

An alternate approach to waveguide techniques is to use quasi-optical coupling where the waveguide horn antenna is replaced by a planar antenna on a thick dielectric substrate that supports the antenna (see review by Rutledge [6] and references therein). The thick dielectric substrate simulates a semi-infinite dielectric half-space thus preventing the propagation of surface modes. Since broadside planar antennas like the bow-tie antenna [7], the logarithmic spiral antenna [8], [9] the double dipole [10] or twin slot antennas [11]–[13] have very broad radiation patterns (typically $f/0.5^*$) the dielectric substrate is shaped to be a hyperhemispherical lens to reduce the beam pattern's width by n [14], where n is the refractive index, yielding $f/1$ to $f/2$ depending on the dielectric used. The hyperhemispherical lens uses the aplanatic focus of a sphere at a distance $d = r/n$ from the center of the sphere where r is the radius of the sphere [15]. The detector, or an impedance matching circuit feeding the detector, receives the power from the apex of the planar antenna.

The advantages of planar-structure antennas compared to waveguide systems are their low cost of manufacture, east of installation, applicability to mass production using photolithographic techniques [6], and lower losses at high frequencies. The down side to this approach is that, so far, lower Gaussian coupling efficiencies have been found [16]–[18], when compared to waveguide horns. Also the beam launched by the hyperhemispherical lens and planar antenna combi-

Manuscript received August 13, 1992; revised March 8, 1993.

The author is with the Division of Physics, Mathematics and Astronomy, California Institute of Technology, Pasadena, CA 91125.

IEEE Log Number 9211932.

* f-numbers in this paper are defined through the FWHP angle—see equation (1).

nation is so broad [12], [16], [17] that additional optics are required to match it to a typical beam ($f/6$ to $f/20$) of a Cassegrain focus telescope. However, earlier work with planar antennas on hyperhemispherical lenses like the bow-tie antenna [16] or logarithmic spiral antenna [17] yielded high receiver sensitivities. This effect of poor coupling but high receiver sensitivity can be understood when the different ways of applying input radiation to the detector are considered. In the case of the coupling efficiency measurements, a single-mode Gaussian beam from the telescope has to be coupled to the receiver antenna, thus the amplitude and phase properties of the receiving antenna's beam are important. For sensitivity measurements, blackbodies are used as sources of radiation in front of the receiver, i.e. between the receiver and the telescope (see Fig. 1). Blackbodies are multi-modal sources, thus all components of the receiver antenna's beam pattern that are not blocked by apertures between the receiver antenna and the outside (such as dewar window, etc.) will receive power from the blackbodies. Therefore these measurements are insensitive to the beam pattern quality and the phase of the receiver's antenna. The beam pattern quality only contributes to the loss of sensitivity through that fraction that is blocked by apertures between the antenna and the blackbodies. Since the log periodic spiral antenna has superior amplitude beam patterns compared to the bow-tie antenna [7], [9], a receiver based on the log periodic spiral antenna [17] naturally showed higher sensitivities than one based on the bow-tie antenna [16]. However, both receiver systems showed relatively poor coupling to a single mode Gaussian beam from a telescope when compared to receiver systems with waveguide horn antennas. This was probably due to problems in the optics resulting from the challenge in matching the very broad beam launched by the planar antenna ($f/0.5$) to the telescope optics (typically $f/6-10$). A more detailed discussion of the reasons for the low Gaussian coupling efficiencies of those previous quasi-optical systems can be found at the end of Section II.

The goal was to develop a quasi-optical antenna system that would allow the receiver to couple to the telescope optics without any degradation, i.e. antennas with high quality beam patterns, high f-numbers and high Gaussian coupling efficiencies. Ideally, no additional optics should be required between the antenna that launches the beam and the telescope optics. The hybrid antenna, introduced in this work, is such an antenna. The new hybrid antenna adds the properties of excellent radiation patterns and high aperture efficiencies to the several existing advantages of planar antennas. The size of the beam can be designed to match the requirements (e.g. $f/4$ to $f/20$) without any additional optics between the receiver antenna and the telescope. Furthermore the dielectric antenna is very space efficient, i.e. it has a high aperture efficiency (76%), thus being well suited for heterodyne receiver focal plane array applications. Beam pattern ray calculations including diffraction limit effects are discussed in Section II. An application of a single hybrid antenna in an SIS receiver and considerations for array optics in Section III.

Throughout this work the following four nomenclatures will be used:

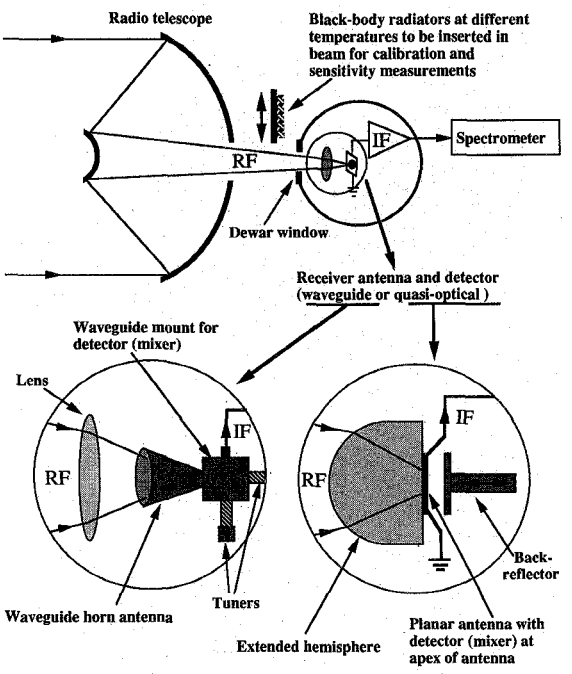

Fig. 1. Optics layout for a radio telescope. The radiation from the telescope is focused onto the detector via a lens and a waveguide horn or a quasi-optical lens system. Loads of different temperatures are inserted in the optical path between the primary dish and the receiver dewar to measure the sensitivity of the system.

1) A dielectric sphere of radius r and refractive index n that is cut off at a plane a distance d from its center is called extended hemispherical lens of extension length d (see Fig. 2).

2) If that extension length is at $d = r/n$, i.e. the lens is aplanatic [15], it is termed a hyperhemispherical lens.

3) When the extension length d is increased beyond the aplanatic point (for a lens with radius larger than a wavelength) the magnification will increase until the diffraction limit of the lens is reached. At that extension length ($d = d_{\text{opt}}$) the diffraction limited lens acts as a lens-antenna and the combination of it with the planar feed antenna mounted on its flat surface is named a hybrid antenna. The planar antenna is then called the feed antenna of the hybrid antenna. The reason for choosing the name hybrid antenna is that it is made of two antennas, a dielectric lens-antenna that defines the beam pattern of the hybrid antenna through the diffraction limit given by the lens-antenna's radius and a planar antenna that defines the polarization properties of the hybrid antenna. Both of the component antennas contribute to the overall radiation properties of the final antenna. A more detailed discussion of the operating principles of the hybrid antenna will follow later.

4) An elliptical lens-antenna is an ellipsoid cut off at a plane perpendicular to its major axis at its second geometric focus, with a planar antenna mounted on the flat surface. Also, throughout this work the following definition for the f-number of an optical system will be used:

$$f-\text{number} \simeq \frac{1}{2\tan(\theta_{\text{FWHP}}/2)}, \tag{1}$$

with θ_{FWHP} the full width at half power (FWHP) angle of the beam.

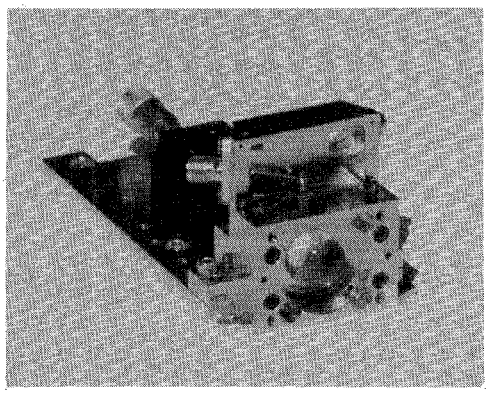

(a)

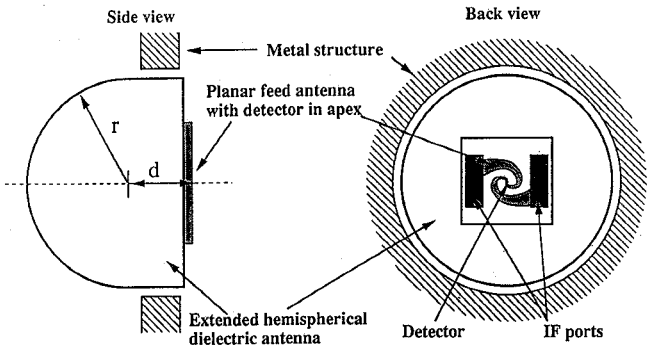

(b)

Fig. 2. (a) Photograph of a hybrid antenna in a mixer block. The anti-reflection coating has been removed to show the dielectric lens antenna of the hybrid antenna in the center of the mixer block. The block is mounted on a base plate that holds the micrometer stage, visible in the background, used to adjust the back plane position. (b) Schematic of a hybrid antenna in a metal structure. The extension length d is defined from the center of the hemispherical dielectric to the metallization of the planar antenna.

Previous measurements of elliptical lens-antennas showed good beam patterns [19], [20] requiring no further optics to couple to a typical Gaussian beam from a telescope, but the important question of Gaussian coupling or aperture efficiency was not addressed. Adding to the known advantages of the elliptical lens-antenna, the hybrid antenna is less expensive to manufacture. The important figure of merit for the hybrid antenna then is the Gaussian coupling efficiency of the system or the aperture efficiency when used in an imaging array receiver. Aperture efficiency measurements of the hybrid antenna, based on total power measurements, and a discussion of Gaussian coupling efficiencies based on calculations and measurements by Filipovic *et al.* [21] will be presented in the next section.

II. Hybrid Antenna Concept, Theory and Properties

Two issues, those of quality of beam patterns and aperture efficiency of the antenna, have to be addressed for an antenna is a quasi-optical imaging array receiver. For a single element receiver the Gaussian coupling efficiency is most important, but in an array receiver the aperture efficiency of the individual antennas is important, since it is a measure of the efficiency in the use of focal plane space with which the antennas sample the incoming radiation. In general, these properties are, of course, related. However, for simplicity they will be treated separately.

A. Physical Description of the Hybrid Antenna

Fig. 2 shows a photograph and a schematic diagram of the hybrid antenna with all accessories as discussed below. Thinking of the antenna as a transmitter, the radiation is fed into the system by a planar antenna that uses the extended dielectric hemisphere as a substrate. Planar antennas suffer from power loss to substrate modes when the dielectric substrate is of comparable thickness to a wavelength, but mounting the planar feed antenna on a substrate lens antenna eliminates this problem by simulating a semi-infinite half-space of dielectric for the planar feed antenna. This also causes the feed antenna to radiate preferentially in the direction of the dielectric. For a dielectric constant of $\varepsilon_r = 3.8$ and a spiral feed antenna, the ratio of power radiated into the dielectric to that radiated to the opposite face was found to be about 7 dB. This ratio depends on the beam width of the planar antenna and will increase for wider beams and higher dielectric constants ε_r [6]. The planar spiral antenna used throughout this work is identical to the one used in [17], which is a two-turn, self-Babinet-complimentary structure, with a diameter of about 3 mm and an opening angle of 30°. A metal back plane on the free space side of the feed antenna was used to reflect forward that power which would otherwise be lost from the beam. To verify that the back reflector does not impact the beam patterns but acts only to recover the power otherwise lost, it was replaced with an absorber. When the back reflector was positioned for peak response, i.e. about $3/8\lambda$ away from the planar feed antenna, the patterns were identical to those measured with an absorber. The back reflector can be eliminated by using a dielectric substrate of very high dielectric constant, such as high resistivity silicon ($\varepsilon_r = 11.7$), since the power radiated into the free space direction is then negligible. However, the transition from the front surface of the dielectric lens-antenna to free space is then more critical, requiring the use of an anti-reflection coating.

B. Beam Pattern Measurements and Concept of the Hybrid Antenna

The beam measurements were performed using a computer controlled full two-dimensional angular far-field scanning antenna range in a microwave absorbing chamber. The source for the 115 GHz measurement was a Gunn oscillator, and for frequencies up to 500 GHz Gunn oscillators followed by multipliers were used. The measurement at 584 GHz used a far infrared laser system for the source. The distance between the source and the hybrid antenna was about 1m. The sources were all linearly polarized and modulated with a chopper wheel. The detector for the power received by the antenna was a bismuth bolometer placed at the apex of the planar antenna [22]. The bolometer was dc-biased and the chopped signal amplified with a lock-in amplifier. The dynamic range of the set-up was about 25 dB. To get a better dynamic range than the one achieved here with room temperature techniques would require the use of different detectors such as

Schottky diodes. However, bolometers were chosen since they could be manufactured lithographically *in situ* with the antenna structure rather than having to mount a separate detector in the apex of the antenna. The size of the bolometers is about 1 μm, enabling the antenna measurements to be performed in the submillimeter band without having the size of the detector affect the characteristics of the antenna system.

The concept of the hybrid antenna is to use the dielectric substrate's lens itself as a radiating aperture antenna by choosing the extension length d of the extended hemispherical lens to be large enough so that the f-number of the lens is increased to the point where, for its particular diameter, the diffraction limit is reached. The beam launched from that position will approximate a wave with constant phase outside the dielectric antenna. Fig. 3 shows measurements of beam patterns as a function of the extension length d of an extended hemispherical lens performed at 115 GHz. The extension length d was increased in the measurements by adding quartz slabs of 0.254 mm thickness between the flat surface of the dielectric lens and the substrate of the planar antenna. The radius r of the dielectric lens antenna used was $r = 6.35$ mm and the refractive index $n = 1.95$ of the fused quartz dielectric. The quality of the patterns increases when the distance d is increased from the hyperhemispherical case of $d = r/n = 3.25$ mm up to the point $d = d_{\text{opt}}^{\text{meas}} = 4.27$ mm where the beam is diffraction limited and the sidelobes are at a minimum. A further increase of d then raises the sidelobe level while the main beam remains diffraction limited.

Fig. 4 shows the excellent beam pattern quality of a hybrid antenna in a two-dimensional linear scale depiction (4a) and two perpendicular cuts in a logarithmic scale depiction (4(b)–(c)). The pattern was taken at 115 GHz with a 12.7 mm diameter fused quartz lens of dielectric constant $\varepsilon_r = 3.8$ with the hybrid antenna mounted in a metal mixer block (see Fig. 2) like the one used in the SIS receiver with a back reflector, as described later. The measurements were performed in a metal mixer block, as encountered in most applications, so as not to exclude the possibility of problems of distortions of the beam pattern arising from the proximity of conducting surfaces to the hybrid antenna. The metal of the mixer block in the configuration used is concentric around the hybrid antenna in the same plane as the planar antenna with a distance from the apex of the planar antenna equal to the radius of the extended hemisphere (see Fig. 2).

To investigate the optimum extension length d_{opt} dependance on wavelength, measurements at 492 GHz were carried out the same way as those described above at 115 GHz shown in Fig. 3. A new optimum, position $d_{\text{opt}}^{\text{meas}}$(492 GHz) was found with $d_{\text{opt}}^{\text{meas}}$(492 GHz) $> d_{\text{opt}}^{\text{meas}}$(115 GHz). This effect can be understood from Fig. 5, which is a geometric ray calculation including the effects of the diffraction limit for a lens of same refractive index and radius as those of the measurements. Defining the angular ratio R_θ as the ratio of the angle of a ray launched by the planar antenna to that of the ray as it leaves the extended hemispherical lens, Fig. 5 shows R_θ as a function of extension length d for a set of different rays launched by the planar antenna. As d increases from zero, i.e. a hemispherical lens, towards the length where

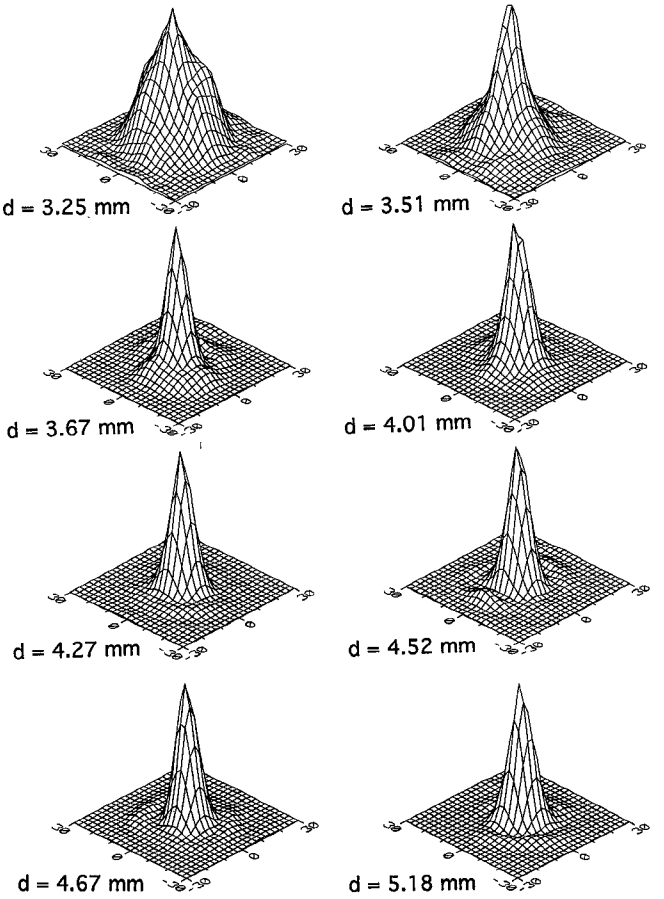

Fig. 3. Beam pattern measurements in linear intensity depiction for different distance parameters d. The radius of the hybrid antenna was 6.35 mm, the dielectric constant $\varepsilon_r = 3.8$ and the frequency 115 GHz ($\lambda = 2.6$ mm). The position of $d = 3.25$ mm corresponds to the aplanatic case (i.e. a hyperhemispherical lens) where $d = r/n$. The measured beam for this position is that of the planar spiral antenna reduced in width by n by the lens. At $d = 4.27$ mm the beam pattern is diffraction limited and a further increase of d only increases the sidelobe levels. This position is the experimentally determined optimum position $d_{\text{opt}}^{\text{meas}}$(115 GHz). The beam pattern is now defined by the radius of the lens rather than the beam properties of the planar feed antenna.

the extended hemispherical lens approximates an elliptical lens at its second geometric ray focus, R_θ increases from unity to infinity. However, for wavelengths λ comparable to the radius r of the lens, geometric ray optics alone is not a good approximation anymore, but requires modification due to the diffraction limit of the lens, which is governed by the radius of the lens. The full width at half power (FWHP) diffraction angle θ_{FWHP} is given by [15]

$$\theta_{\text{FWHP}} \simeq \frac{1.2\lambda}{2r}. \tag{2}$$

In Fig. 5 the positions where this diffraction angle is reached for the ray leaving the extended hemisphere are denoted by boxes for 115 GHz (2.6 mm) and circles for 492 GHz (0.61 mm). The dotted and dash-dotted line connect those points and were calculated using a larger sample of rays launched by the planar antenna. The important feature to note is that there is an extension length $d_{\text{opt}}^{\text{calc}}$ beyond which it is not necessary to increase d since every ray launched by the feed antenna is either already within the diffraction limit (given by

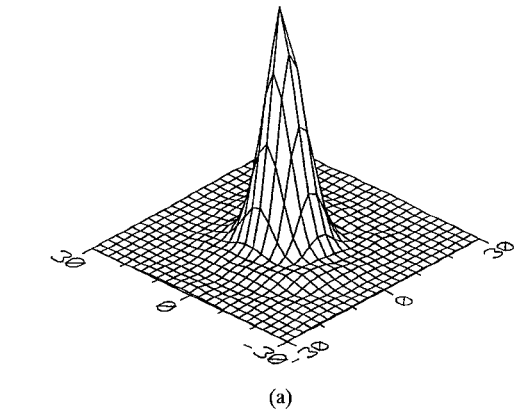

(a)

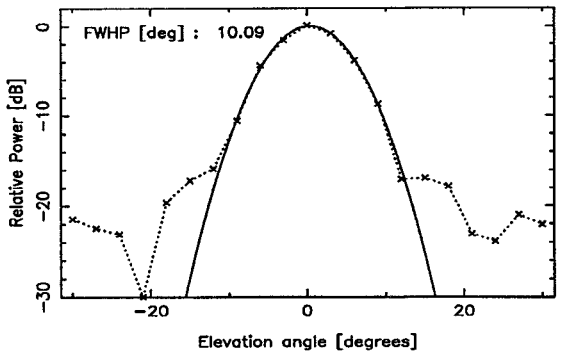

(b)

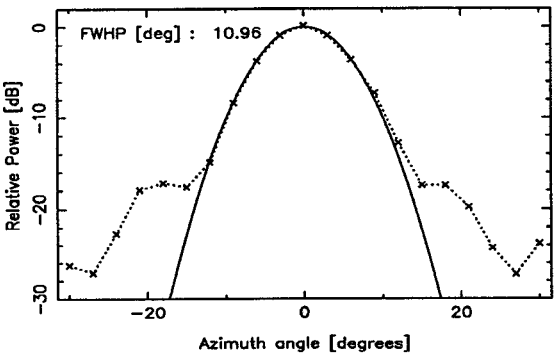

(c)

Fig. 4. Beam pattern of a hybrid antenna with $\varepsilon_r = 3.8, r = 6.35$ mm, $d = d_{\rm opt}^{\rm meas} = 4.27$ mm at 115 GHz. (a) the full two-dimensional pattern on a linear scale. (b) and (c) two perpendicular cuts with a logarithmic intensity scale. The solid line is a best fit Gaussian profile and matches the measured data very well down to about -17 dB.

(2)) of the beam leaving the hybrid antenna or is refracted into it by the extended hemispherical lens, as demonstrated in Fig. 5.

The calculated optimum extension length $d_{\rm opt}^{\rm calc}$ can be determined numerically from graphs as the ones shown in Fig. 5. Fig. 6 shows a plot of the ratio $d_{\rm opt}^{\rm calc}/r$ versus the radius of the lens r measured in units of wavelength. Comparing the calculated and measured optimum positions one finds them to agree very well and the results are listed in Table I.

A hybrid antenna that is to cover a wide range of frequencies must use a $d_{\rm opt}(\mathrm{F}_h)$ as determined for the highest frequency F_h. As shown later (see Table IV) the aperture efficiency at the lowest frequency F_l will then be slightly lower than the optimum attainable for that frequency, since $d_{\rm opt}(\mathrm{F}_h) > d_{\rm opt}(\mathrm{F}_l)$. However, unless the operating range is more than

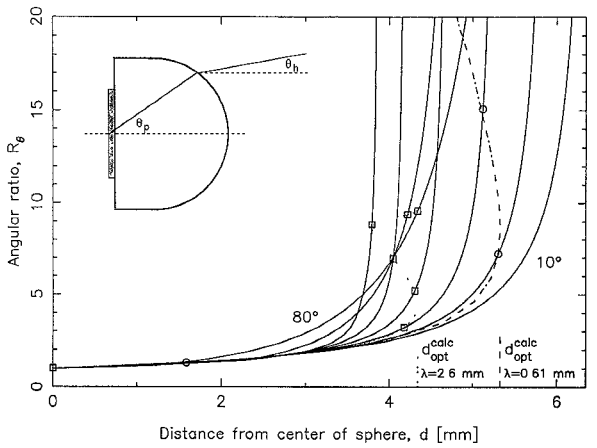

Fig. 5. Geometric ray calculations including the diffraction limit for hybrid antennas. The angular ratio is the ratio of an angle θ_p of a ray as launched by the planar antenna inside the dielectric to the angle θ_h of the ray launched by the hybrid antenna (see insert in upper left corner). This ratio increases monotonically with increasing distance d of the position of the planar antenna to the center of the extended hemispherical lens. Rays are shown (solid lines) starting at an angle $\theta_p = 10°$ with increments of 10° up to 80°. The intersection of the dotted line ($\lambda = 2.6$ mm or 115 GHz) and dash-dotted line ($\lambda = 0.61$ mm or 492 GHz) with the solid lines indicate where the angular ratio is large enough to have the ray, as launched by the hybrid antenna, to be within the diffraction limit of the dielectric lens antenna. For a distance $d = d_{\rm opt}$ (indicated by the dotted and dashed-dotted vertical lines) all rays launched by the planar antenna are within the diffraction limit. This position depends on the wavelength through the diffraction limit. Beam pattern measurements, as shown in Fig. 3 for 115 GHz agree very well to the $d_{\rm opt}^{\rm calc}$ (F) predicted by the calculations shown in this figure.

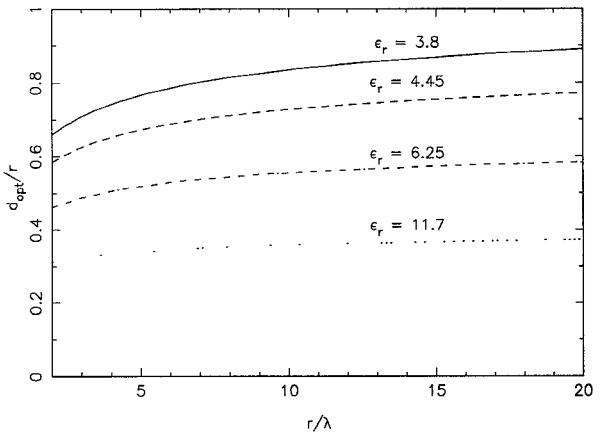

Fig. 6. The optimum extension length as a fraction of the radius of the lens, $d_{\rm opt}^{\rm calc}/r$, as function of radius of the lens measured in units of wavelength, r/λ, for different dielectric constants ($\varepsilon_r = 3.8$: fused quartz, $\varepsilon_r = 4.45$: single crystal quartz, $\varepsilon_r = 11.7$: high resistivity silicon). The geometric ray method of Fig. 5 was used to generate the results shown here. A hyperhemispherical lens would yield a flat line at $1/\sqrt{\epsilon_r}$.

TABLE I
COMPARISON OF CALCULATED TO MEASURE OPTIMUM EXTENSION LENGTH $d_{\rm opt}$

frequency/Wavelength	115 GHz/2.6 mm	492 GHz/0.61 mm
calculated: $d_{\rm opt}^{\rm calc}$	4.33 mm	5.34 mm
measured: $d_{\rm opt}^{\rm meas}$	4.3 ± 0.2 mm	5.4 ± 0.2 mm

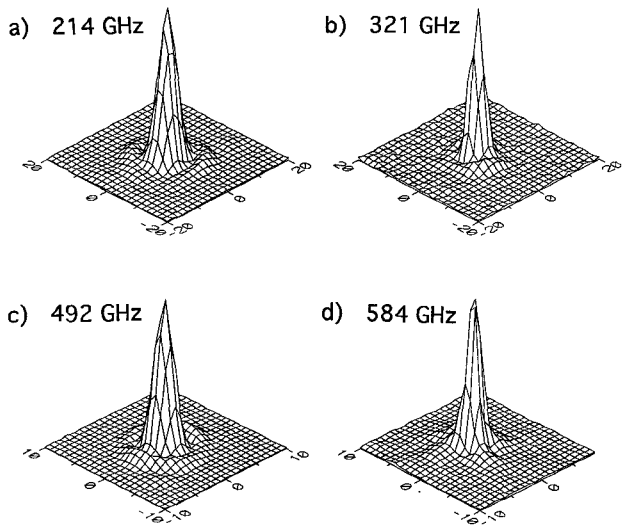

Fig. 7. Beam patterns of hybrid antennas at different frequencies. (a) 214 GHz, $\varepsilon_r = 3.8$, $r = 6.35$ mm, $d = 5.18$ mm ($d_{\text{opt}}^{\text{calc}} = 4.80$). (b) 321 GHz, $\varepsilon_r = 3.8$, $r = 6.35$ mm, $d = 5.18$ mm ($d_{\text{opt}}^{\text{calc}} = 5.07$). (c) 492 GHz, $\varepsilon_r = 3.8$, $r = 6.35$ mm, $d = 5.44$ mm ($d_{\text{opt}}^{\text{calc}} = 5.33$). (d) 584 GHz, $\varepsilon_r = 4.45$, $r = 10.0$ mm, $d = 8.01$ mm ($d_{\text{opt}}^{\text{calc}} = 7.71$). The extension length d was not optimized in these measurements, but set to have $d(\text{F}) \geq d_{\text{opt}}^{\text{calc}}(\text{F})$.

an octave, the reduction in aperture efficiency is typically well under 10%.

Fig. 7 shows beam pattern measurements at 214, 321, 492 and 584 GHz for hybrid antennas with $d(\text{F}) \geq d_{\text{opt}}^{\text{calc}}(\text{F})$. The 214 and 321 GHz measurements used low efficiency multiplies to generate the transmitter signal, thus the lower signal to noise levels. The 492 GHz and 584 GHz measurements yielded signal to noise ratios as good as in the 115 GHz measurements due to narrower beams and higher available transmitter power using a high efficiency Gunn multiplier chain [23] and a far infrared laser system, respectively.

C. Calculated Reduction of Aperture Efficiency from Phase Errors

In the limit of very high frequencies and large lens sizes, i.e. the geometric ray approximation, the hybrid antenna would approach that equivalent to the second geometric ray focus of an ellipsoid of revolution. For these conditions it would be advantageous to actually use an elliptical lens rather than an extended hemispherical lens. In the geometric ray approximation an elliptical lens focuses parallel light to a single point within the lens, i.e. with no aberrations, whereas an extended hemispherical lens will have some aberrations (see Figs. 8 and 9). However, in those cases where the lens size is not much larger than the operating wavelength, an elliptical lens can be approximated with a much lower cost extended hemispherical lens, which was done in all measurements of this work. The reduction of aperture efficiency, due to phase errors in the aperture plane, for an extended hemisphere versus a truncated elliptical lens, depends on the diameter of the lens, the wavelength and the refractive index of the lens material. Fig. 8 shows the phase fronts as calculated with geometric ray optics for two different 12.7 mm diameter lenses with a refractive index of $n = 1.95$ at 500 GHz. One lens is a truncated ellipsoidal lens where the wavefront and lens are shown by solid lines and the other lens is an extended hemispherical lens with wavefront shown as dashed lines. The dotted line shown in Fig. 8 is the difference between the wavefront of the ellipsoidal lens and the extended hemispherical lens after a quadratic term for refocusing was removed. The parameter d of the extended hemispherical lens is $d = d_{\text{opt}}^{\text{calc}} = 5.34$ mm as determined from Fig. 5. The elliptical lens has the same length of its minor axis b as the radius r of the hemisphere. The (x) symbols denote the foci of the ellipse, which are a distance $c = a/n$ from the center (+) of the ellipse. The major axis a of the ellipse is then determined from $a^2 = c^2 + b^2$. The circle (o) denotes the center of the spherical lens. The aperture efficiency loss due to the phase error $\chi(\rho, \phi)$ is calculated from

$$A_{\text{loss}}^{\text{phase}} = 1 - \left|\left\langle e^{i\chi}\right\rangle\right|^2 = 1 - \frac{\left|\int_0^{2\pi}\int_0^r e^{i\chi(\rho,\phi)}\rho\, d\rho\, d\phi\right|^2}{\left[\int_0^{2\pi}\int_0^r \rho\, d\rho\, d\phi\right]^2} \tag{3}$$

and is about 10%. The electric field is assumed to be constant in amplitude across the aperture. The onset of sidelobe shoulders at about -17 dB, as shown in Fig. 4(b) and (c), is a typical signature of an Airy pattern from the constant illumination in phase and amplitude [15] of a circular aperture and are consistent with the above assumption. However, it is important to stress that there can be very different illumination functions that will still produce beams with sidelobes at -17 dB. Most of the phase errors occur at the edges of the aperture as can be seen in Fig. 8. Since different planar antennas will yield different illumination functions, especially at the edges, a constant amplitude in the aperture plane was chosen. This was done to simplify comparison of the different parameters of Fig. 9. A constant amplitude in the aperture plane corresponds to a FWHP beam angle for the planar antenna inside the dielectric of about $f/0.5$. Again, a quadratic term in the phase front was removed for Fig. 9 since this reflects only a different focusing position. The ratio of the radius r of the lens to the wavelength λ is proportional to the f-number of the hybrid antenna, since from (1) and (2)

$$f - \text{number} \simeq \frac{1}{2\tan\left(\frac{0.3\lambda}{r}\right)} \tag{4}$$

Fig. 9 shows the calculated reduction in aperture efficiency at a function of r/λ for different refractive indices. The reduction in aperture efficiency increases with increasing size of the lens since the approximation of an extended hemispherical lens to an elliptical lens becomes worse, which will increase aberrations. A higher dielectric lens will have less aberrations since an elliptical lens of that material will be closer to a sphere. The extended hemispherical lens is thus a better approximation to the elliptical lens.

Table II summarizes beam pattern measurements performed between 115 GHz and 492 GHz with dielectric antennas of two different diameters: 6.35 mm and 12.7 mm. Measurements done at 584 GHz are not listed since the lens used for

TABLE II
BEAM PATTERN MEASUREMENTS SUMMARY

diam. [mm]	freq. [GHz]	FWHP (E)	FWHP (H)	$f\#$	$f\# \cdot \lambda$ [mm]
6.35	115	20.3	17.8	3.0	7.8
6.35	208	11.6	11.3	5.0	7.2
6.35	492	4.86	5.39	11.2	6.8
12.7	115	10.9	10.2	5.4	14.1
12.7	208	5.4	6.3	9.8	14.2
12.7	214	4.9	6.1	10.4	14.6
12.7	321	4.0	4.1	14.2	13.3
12.7	428	2.85	2.91	19.9	13.9
12.7	492	2.92	2.52	21.1	12.8

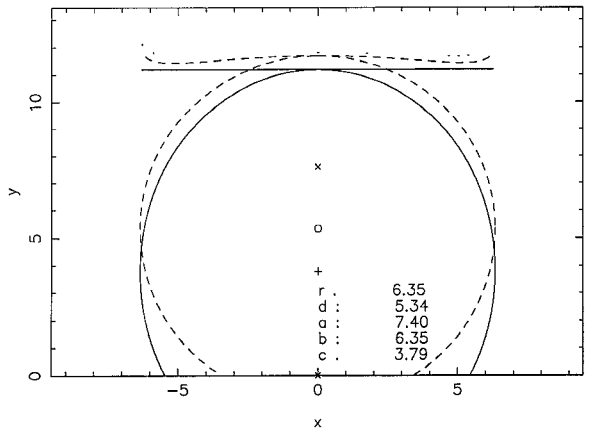

Fig. 8. Truncated ellipsoidal lens with wavefront (solid lines) and extended hemispherical lens with wavefront (dashed line) from geometric ray optics calculations. The dotted line is the difference between the wavefront of the ellipsoidal lens and the extended hemispherical lens after a quadratic term for refocusing was removed. The radius of the extended hemispherical lens is $r = 6.35$ mm, $\varepsilon_r = 3.8$ and $d = d_{\text{opt}}^{\text{calc}} = 5.34$ mm as determined from Fig. 5. The elliptical lens has the same length of its minor axis b as the radius r of the hemisphere. The (x) symbols denote the foci of the ellipse, which are a distance $c = a/n$ from the center (+) of the ellipse. The major axis a of the ellipse is then determined from $a^2 = c^2 + b^2$. The circle (o) denotes the center of the spherical lens.

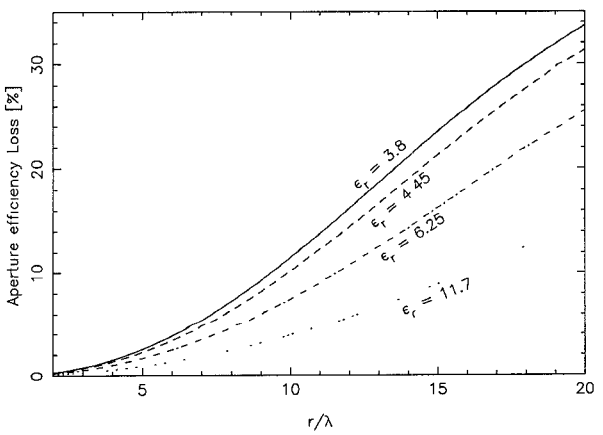

Fig. 9. Calculations of loss of aperture efficiency due to phase errors of an extended hemispherical lens as a function of the ratio of the radius of the lens to the wavelength, r/λ, for different dielectric constants ($\varepsilon_r = 3.8$: fused quartz, $\varepsilon_r = 4.45$: single crystal quartz, $\varepsilon_r = 11.7$: high resistivity silicon). A uniform amplitude in the aperture plane was chosen.

those measurements (20 mm diameter) was from a different supplier and had significant surface errors resulting in aberrations which dominated the measurement results. The beam size is given as the full width at half power (FWHP) in the E-plane and H-plane of the transmitting horn antennas. The $f\#$ is calculated from the geometric mean FWHP angle θ_{FWHP} via (1) and (2). The product, $f\# \cdot \lambda$, yields the spot size in the image plane and should correspond to the diameter of the dielectric lens-antenna, if the antenna behaves as a diffraction limited, uniformly illuminated aperture. As shown in Table II, this is approximately the case for all the measurements. However, Table II shows a general trend for $f\# \cdot \lambda$ to decrease with increasing frequency. By inspection, it can easily be verified that this is not due to the tan-function affecting the low f-number results more than the high f-number results. The systematic decrease of $f\# \cdot \lambda$ is attributed to an increase in the measured beam width due to increasing phase errors. In addition to the phase errors discussed previously, there could be phase errors from surface inaccuracies of the lens. The lenses used have a surface accuracy of better than 2 μm. The loss of coupling efficiency L can be estimated from the Ruze [24] formula for telescopes, modified for a lens with refractive index n:

$$L = 1 - e^{-(2\pi(n-1)E_{\text{RMS}}/\lambda)^2}, \tag{5}$$

which is negligible at submillimeter wavelengths for $E_{\text{RMS}} \approx 2\mu$m. It is thus concluded, that the slightly increased beam sizes are caused by phase errors from aberrations as discussed in the text accompanying Figs. 8 and 9.

D. Aperture Efficiency Measurements

Beam pattern measurements can usually be performed rather easily whereas aperture and Gaussian coupling efficiency measurements require absolute power calibration, which can be difficult at millimeter and submillimeter wavelengths. Laboratory measurements at 115 GHz with a planar-logarithmic-spiral-structure as the feed antenna of a hybrid antenna were performed and an aperture efficiency of $(76 \pm 6)\%$ was obtained. These measurements were performed at room temperature with a bismuth bolometer at the apex of the planar feed antenna. The manufacture of the bismuth bolometers and their responsivity calibration have been described by Neikirk *et al.* [22]. The measured aperture efficiency depends on absolute power measurements done with the bolometer, which was thermally calibrated with direct currents provided through the bias circuit.

For the RF measurements the extended hemisphere was covered with a quarter-wave-anti-reflection coating to avoid reflection from the dielectric surface, and the back reflector was positioned for maximum response. In the design presented here, the hybrid antenna is fed by a planar logarithmic spiral antenna, which accepts elliptical polarization [17]. The polarization of the hybrid antenna is therefore elliptical too. The transmitter used a standard gain horn with linear polarization. Two measurements with the transmitter horn rotated by 90° were performed and the received power from both measurements was added together. The difference between the received power for the two perpendicular linear polarizations of the transmitter measurements was less than 10% showing that the hybrid antenna with a logarithmic spiral antenna is nearly circularly polarized, i.e. the eccentricity of the elliptical polarization is small. By adding the power of the two polarization measurements together the hybrid antenna's circular co-polarized component is added to the circular cross-polarized component. In millimeter and submillimeter wavelengths radio astronomy the signal is typically randomly polarized so that the addition correctly yields the aperture efficiency as appropriate for a radio-astronomical receiver. However, some receivers—like Schottky diode receivers, which require high local oscillator power levels—may have polarizing optics in front of the mixer eliminating one polarization of the signal.

No correction was made for any mismatch between the antenna impedance and the bolometer, since the resistance of the feed antenna's arm material was not well known and the bolometer's resistance could not be measured without the feed antenna in series. The thickness of the antenna arms was approximately 0.2 μm and RF losses due to the surface resistance of the antenna arms were also not taken into account. The actual efficiency will therefore be higher than quoted here. However, these effects are estimated to be less than 5%.

Subsequent to the measurements discussed here, efficiency and beam pattern measurements using planar Schottky diodes soldered into the apex of a logarithmic periodic antenna at 90 GHz and 180 GHz (G. Rebeiz, private communication, 1991) and with a double slot antenna at 246 GHz [21] were performed. They confirmed the measurements of this work with higher signal to noise levels for the pattern measurements and calculated similar aperture efficiencies from the pattern measurements.

To calculate the aperture efficiency from the received and transmitted power, P_r and P_t respectively, Friis' transmission formula [25] is solved for the effective aperture of the hybrid antenna

$$A_e = \frac{P_r}{P_t}\frac{\ell^2\lambda^2}{A_{et}}, \tag{6}$$

with ℓ the distance between the transmitting antenna and the receiving hybrid antenna, and A_{et} the effective aperture of the transmitting antenna. The physical aperture of the hybrid antenna with a lens radius of $r = 6.35$ mm is $A_p = \pi r^2 = 127$ mm^2. The effective area of the transmitting antenna, a standard gain horn (Alpha Ind., model F861-33), was calculated [26] and also measured in a symmetric (transmit/receive) setup using two identical standard gain horns. The effective area of the horn was found to be $A_e(\text{horn}) = (142 \pm 9)$ mm^2. The effective area of the hybrid antenna is

$$A_e(\text{hybrid}) = (95 \pm 7) \text{ mm}^2 \tag{7}$$

and thus for the aperture efficiency

$$\eta_a = 0.76 \pm 0.06. \tag{8}$$

The error in the measurement is mostly due to the uncertainty in the measurement of the effective area of the transmitting horn antenna (1σ: 6%) and the absolute power calibration of the bolometer (1σ: 5%). Also, note that all measurements were made in a realistic environment for the hybrid antenna, i.e. in a metal mixer block rather than idealized conditions.

For applications requiring only one polarization, the cross polarized power would have to be subtracted, reducing the aperture efficiency by that fraction. Using a linearly polarized planar logarithmic periodic antenna as the feed antenna for the hybrid antenna, a maximum cross-polarized beam of -7 dB relative to the co-polarized beam was found. However, the cross-polarized component of a log-periodic antenna has been found to vary with frequency [27] and lies between -5 and -15 dB. The cross-polarized beam pattern followed the co-polarized pattern so that it only reduces the aperture efficiency for applications with a singly polarized source. If linear polarization is a requirement for a particular application but multi-octave bandwidth can be sacrificed, work by Zmuidzinas and LeDuc [12] and Rogers ad Neikirk [13] with a double slot antenna suggests that this planar antenna is a good choice as a feed antenna for a hybrid antenna. This was recently verified by Filipovic *et al.* [21], who made beam pattern measurements of a hybrid antenna with high dynamic range (40 dB) thus allowing them to calculate the aperture efficiency. The calculation yielded an aperture efficiency of $(73 \pm 5)\%$ for a hybrid antenna with a twin slot feed antenna at 246 GHz, which is in good agreement with the results of this work.

E. Comments on the Gaussian Coupling Efficiency

From theory, using ray-tracing inside the dielectric lens and electric and magnetic field integration on the spherical surface of the lens, Filipovic *et al.* [21] find the Gaussian coupling efficiency (GCE) of the hybrid antenna reduced by about 8% compared to a hyperhemisphical lens (the aplanatic, thus aberration-free case, of an extended hemispherical lens) system, which they calculate to have a GCE of 97%. However, they were unable to experimentally verify the higher GCE for the aplanatic optics but rather measured a lower GCE (87%) for the aplanatic case compared to the hybrid antenna case (GCE $\simeq$ 89%). The reasons are probably the same as in the case of earlier receivers with aplanatic hyperhemispherical lenses which showed poor coupling to a single Gaussian mode of a telescope, as mentioned above. In the case of receivers this effect was even stronger than for the measurements of Filipovic *et al.*. Filipovic *et al.* used room temperature optics that were optimized, yielding focusing parameters different from the ones predicted by Gaussian optics calculations, whereas the receiver optics with cryogenically cooled SIS

detectors allow for much less optimization thus possibly yielding much worse results. The discrepancy between the optimized positions of components in the experiment and their calculated positions using Gaussian optics are most likely due to the Gaussian optics formalism breaking down for very low f-numbers as are encountered in the optics of the aplanatic hyperhemispherical lens. In addition to optimizing the position of optical components the shape of the lenses used to couple the power from the transmitter to the hyperhemispherical lens would also have to be optimized, which was not done, causing lower GCE. Note that all above GCE values are only relative since Filipovic *et al.* did not carry out any total power measurements but normalized the measured GCE to calculate ones for an extension length they call the simulated elliptical lens position, which they derive from geometric ray considerations not including wavelengths effects.

In conclusion, the GCE of the hybrid antenna is high with about 89% (ignoring reflections of the surface of the lens) and possibly close to the best achievable for an extended hemispherical lens system without complex optics following it. This allows good coupling of a hybrid antenna based receiver to a single mode beam from a radio astronomical telescope, as verified at the Caltech Submillimeter Observatory (CSO) at 345 and 492 GHz [28], [29].

III. Applications of a Hybrid Antenna and Considerations for Arrays

A. Application of a Single Hybrid Antenna in an SIS Receiver

A single hybrid antenna was successfully tested at the Caltech Submillimeter Observatory (CSO), a 10.4 m diameter submillimeter telescope on Mauna Kea, Hawaii, in an application with a superconducting insulator superconductor (SIS) detector in heterodyne mode and an RF matching circuit integrated on the arms of a planar logarithmic spiral feed antenna [30]. Aperture, main beam and forward efficiencies of the radio telescope with a hybrid antenna based receiver [28] and scalar-feed horn waveguide receiver systems [1], [31] were measured at 345 GHz and 492 GHz. When the respective efficiencies were compared between the hybrid antenna based receiver and the waveguide horn based receiver, they were found to be identical with the measurement uncertainties ($< 10\%$). These efficiencies include the coupling efficiency between the telescope and the receiver, besides other factors, which depend on the telescope performance, that are constant at each frequency when one receiver is replaced with another one. Since the telescope performance, independent from the receiver coupling, is not well known an absolute efficiency for the receiver coupling to the telescope can not be deduced. Thus, the only conclusion that can be drawn is that the coupling of the hybrid antenna based receiver to a single mode Gaussian beam from a telescope is about the same as that of a scalar-feed horn waveguide receiver. This is the first quasi-optical receiver tested on a radio astronomical telescope to achieve such good performance. Fig. 10 shows a double sideband spectrum taken in the core of the Orion molecular cloud (OMC-1) with the two sidebands centered

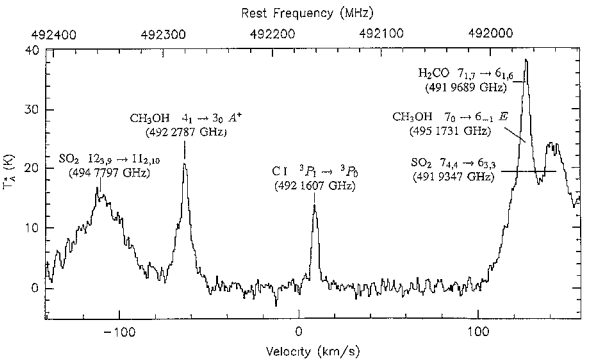

Fig. 10. Submillimeter spectrum of the core of the Orion molecular cloud towards IRc2 taken with a Superconducting-Insulator-Superconductor (SIS) receiver utilizing a hybrid antenna. The data were taken with the 10.4 m aperture telescope of the Caltech Submillimeter Observatory (CSO), Hawaii. The response of two sidebands, centered at 492.16 GHz and 494.96 GHz, is included. The hybrid antenna receiver was compared to waveguide based receivers and yielded similar results for coupling to the telescope and overall telescope efficiencies.

TABLE III
Receiver Noise Temperatures

Frequency [GHz]	318	395	426	492
T_{Rx} (DSB) [K]	200	230	220	500

at 492.16 GHz and 493.66 GHz [29]. Note that the good coupling between the hybrid antenna and the telescope optics is due to the high quality beam patterns of the hybrid antenna and is not necessarily a statement about the intrinsic efficiency of the hybrid antenna itself. The hybrid antenna's coupling efficiency affects the sensitivity of the receiver. Table III shows the sensitivities obtained with the receiver system, expressed in double sideband noise temperatures. The sensitivities obtained are very high and approach those of the best waveguide receivers [1, 31]. The increase of noise temperature at 492 GHz is due to the fact that the lithographic matching circuit, which is designed to tune out the SIS junction capacitance, rolls off at about 475 GHz [30].

The very high sensitivities obtained with the receiver are an indication that the intrinsic coupling efficiency of the hybrid antenna is high. However, it was not possible, as is usually the case, to quantify the coupling efficiency of the hybrid antenna from the noise temperature measurements. The coupling efficiency is just one of many parameters that determine the receivers sensitivity, most of which are not easily measured to better than 10%.

B. Considerations for Array Optics

An antenna that is to be used as an element in a heterodyne array receiver must have several features in addition to being a good single element. Its aperture efficiency has to be high to efficiently sample the image plane, the beam width should be narrow and preferably matched to the telescope optics without further optics, ad finally, the cost and east of manufacture has to be reasonable if large arrays are anticipated.

Table IV shows the aperture efficiencies as determined from total power measurements and the beam widths as determined from the pattern measurements as function of extension length

TABLE IV
APERTURE EFFICIENCIES η_A FOR DIFFERENT LENS EXTENSION LENGTH d MEASURED AT 115 GHZ

Extension d [mm]	3.25	3.51	3.76	4.01	4.27	4.52	4.67	5.18
Mean FWHP [°]	24 ± 3	17.2 ± 1.7	10.8 ± 0.5	11.2 ± 0.5	10.5 ± 0.5	10.2 ± 0.5	10.5 ± 0.5	10.0 ± 0.5
η_A [%]	18 ± 2	29 ± 3	58 ± 7	65 ± 7	76 ± 6	67 ± 7	66 ± 6	71 ± 7

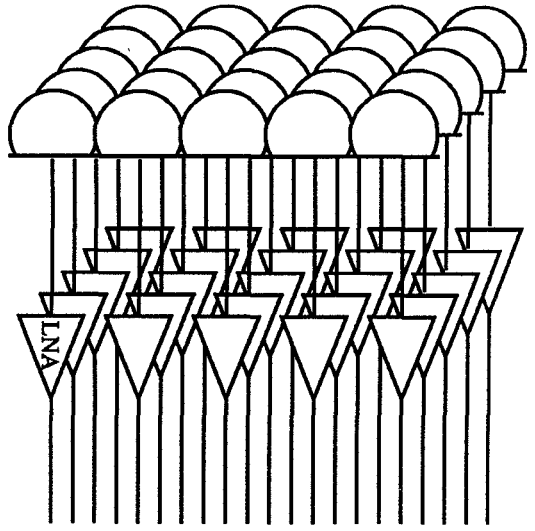

Fig. 11. "Fly's-eye" configuration of a 5 by 5 focal plane array of hybrid antennas. The array of antennas is shown feeding an array of intermediate frequency (IF) low noise amplifiers (LNA). The shown array would be about 35 mm on a side for a telescope with an $f/13$ beam at 492 GHz.

d. The aperture efficiency peaks at the optimum extension length d_{opt}, which is determined experimentally (Fig. 3) and theoretically (Figs. 5 and 6). The lower aperture efficiency, for extension lengths d smaller than d_{opt}, are due to the increase in beam size (i.e. lower directivity), whereas from theory the Gaussian coupling efficiency is expected to increase towards the aplanatic case ($d = r/n = 3.25$ mm), due to smaller aberrations [15]. However, as discussed earlier, Gaussian coupling efficiencies are experimentally typically found to be lower for the aplanatic case [16], [17], [21].

The hybrid antenna in a fly's-eye configuration (see Fig. 11) is considered a good candidate for a single element of an array. Hybrid antennas have high aperture efficiencies and diffraction limited beams, thus can sample the image plane at a spatial frequency of half the Nyquist sampling rate, i.e. undersampled by a factor of two. Planar antennas, which are the feed antennas for hybrid antennas, are inexpensive and easy to manufacture lithographically. The extended hemispherical or elliptical lenses can be manufactured from a mold since the surface accuracy requirements in the millimeter and submillimeter wavelength ranges do not require optical quality finish. To keep the power loss due to surface inaccuracies below 1%, the RMS surface error, as determined from (5), has to be better than $\lambda/20\pi(n-1)$, which is about 10 μm at 500 GHz for a quartz lens.

It is important to note that if the receiver is operated in a total power mode, the image plane has to be sampled at twice the rate (for each linear dimension) compared to a mode where the electric field with its phase is measured (see for example [6]). Radio astronomical receivers used for single telescope observations are typically operated in a total power mode (e.g. autocorrelator spectrometers produce power spectra), despite the fact that, in principle, they are heterodyne receivers and measure amplitude and phase, i.e. they are field sensitive. This implies that a two dimensional array receiver in power detection mode requires four times as many detectors as one that preserves the electric field with the phase information until the image is reconstructed.

At considerable reduction in Gaussian coupling efficiency, the size of the receiving antenna could be made half the linear size of the diffraction limit for field detection, or one-quarter the linear size for power detection, to allow for Nyquist sampling. This is often done for optical systems that are background noise limited. However, in broadband (IF) millimeter and submillimeter wavelength heterodyne receivers, the detector's sensitivity typically determines the overall system sensitivity. Reducing the size of the antenna would reduce the amount of power received by it. Since the noise power produced by the detector stays constant, the signal to noise ratio will suffer. The quadratic relation between the integration time required to achieve a certain signal to noise ratio and the system's sensitivity thus rules out this approach as long as the system's sensitivity remains detector limited.

In this paragraph the reason for suggesting the fly's-eye configuration over a single lens system will be discussed. Measurements of individual planar feed antennas on one big hyperhemispherical lens, i.e. in the aplanatic focus position, showed poor beam patterns for the off-axis elements [32]. A lens with 4λ diameter showed significant distortions of the main beam when operated $1/4\lambda$ off axis and sidelobe levels as high as -4 dB were present when operated $1/2\lambda$ off axis. However, Gaussian coupling efficiencies could still be reasonable high despite some distortions of the main beam. Measurements of an array of feed antennas on an extended hemispherical or elliptical lens, i.e. as a hybrid antenna with an array of feed antennas, were not performed. Since the required size of a single lens to accommodate an array with low distortions would produce beams too narrow to match directly to typical f-numbers of a telescope this approach was not chosen. However, for arrays with few elements, feeding telescopes with relatively high f-numbers, this would be a possible configuration (see for example [20]). In the opinion of the author, the fly's-eye technique is more versatile since it does not restrict the number of elements in the array (the feed antennas are usually fairly big due to the IF and DC connection pads), allowing for the size of the beam to be designed to directly match the beam from a telescope, and allowing all elements of the array to perform equally. Systems that do not provide for a direct match to the telescope optics may suffer from losses introduced from the additional optics

required to match the beams. The hybrid antenna in the fly's-eye configuration avoids these problems. Additionally, the size of the feed antenna is much smaller than the size of the hybrid antenna, thus easily providing room for IF connections or circuits at each element of an array.

IV. Conclusions

Beam pattern and aperture efficiency measurements of hybrid antennas were performed and hybrid antennas are found to be good candidates for focal plane imaging array receivers. Calculations based on geometric ray optics including diffraction limit effects were presented and showed excellent agreement with measurements thus providing all necessary parameters to design hybrid antennas. The manufacture of hybrid antennas is low cost and allows for mass production in arrays. Due to the hybrid antennas' diffraction limited performance they will allow half Nyquist sampling rate (undersampled by a factor of two) of the image plane for field detection or half that sampling rate for power detection. Depending on the application, the feed antenna can be chosen to be a broad band antenna (several octaves) like logarithmic spiral antennas with circular polarization, or a logarithmic periodic antenna with linear polarization. The f-number of the beam can be custom designed to match the optics of a telescope directly. The feed antenna is smaller than the hybrid antenna itself thus ample room for IF connections or circuitry is available at each array element.

Using a planar logarithmic spiral antenna for the feed of the hybrid antenna, an aperture efficiency of 76% was measured. The hybrid antenna was tested in an SIS receiver with a $Nb/AlO_x/Nb$ tunnel junction and a broad band matching circuit yielding coupling efficiencies to a telescope as high as those obtained with corrugated feed horn based receiver systems and sensitivities approaching those of the best waveguide receivers for submillimeter wavelengths.

Acknowledgment

I would like to thank Gabriel Rebeiz, Daniel Filipovic and Brian Kormanyos for their scientific cooperation and Jonas Zmuidzinas, David Rutledge, Chris Walker and Tom Phillips for useful discussions. Chris Walker's help with the construction of the beam pattern measurement system is appreciated. I am indebted to Ron Miller at AT&T Bell Laboratories for supplying the bismuth bolometers and David Rutledge and his group at Caltech for supplying pieces of hardware for the antenna range and for providing the facilities to manufacture the bolometers used initially. The measurements at 584 GHz used a far infrared laser built and operated by Geoffrey Blake for which I am very grateful. This work was supported by grants NSF AST 90-15755 and NASA NAGW-107.

References

[1] B. N. Ellison, P. L. Schaffer, W. Schaal, D. Vail, and R. E. Miller, "A 345 GHz SIS receiver for radio astronomy," *Int. J. of IR and MM Waves,* vol. 10, no. 8, 1989.

[2] G. M. Rebeiz, D. P. Kasilingam, P. A. Stimson, Y. Guo, and D. B. Rutledge, "Monolithic millimeter-wave two-dimensional horn imaging arrays," *IEEE Trans. Antennas Propagat.,* vol. 38, pp. 1473–1482, 1991.

[3] G. V. Eleftheriades, W. Y. Ali-Ahmad, L. P. Katehi and G. M. Rebeiz, "Millimeter-wave integrated-horn antennas, Part I: Theory," *IEEE Trans. Antennas Propagat.,* vol. 39, no. 11, pp. 1575–1581, 1991.

[4] W. Y. Ali-Ahmad, G. V. Eleftheriades, L. P. Katehi and G. M. Rebeiz, "Millimeter-wave integrated-horn antennas, Part II: Experiment," *IEEE Trans. Antennas Propagat.,* vol. 39, no. 11, pp. 1575–1581, 1991.

[5] C. K. Walker, private communication 1991.

[6] D. B. Rutledge, D. P. Neikirk, D. P. Kasilingam, "Integrated circuit antennas," in *Infrared and Millimeter Waves,* vol. 10, pp. 1–90, K. J. Button, Ed., New York: Academic Press, 1983.

[7] R. C. Compton *et al.,* "Bow-tie antennas on a dielectric half-space: Theory and experiment," *IEEE Trans. Antennas Propagat.,* vol. 35, pp. 622, 1987.

[8] V. H. Rumsey, "Frequency independent antennas," in *1957 IRE National Convention Rec.,* pt. 1, pp. 119–128.

[9] J. D. Dyson, "The equiangular spiral antenna," *IRE Trans. Antennas Propagat.,* vol. AP-7, pp. 181–187, Apr. 1959.

[10] D. F. Filipovic, W. Y. Aliahmad, and G. M. Rebeiz, "Millimeter-wave double-dipole antennas for high gain integrated reflector illumination," *IEEE Trans. Microwave Theory Tech.,* vol. 40, no. 5, pp. 962–967, 1992.

[11] A. R. Kerr, P. H. Siegel, and R. J. Mattauch, "A simple quasi-optical mixer for 100-200 GHz," in *IEEE MTT-S Int. Symp. Dig.,* pp. 96, Apr. 1977.

[12] J. Zmuidzinas and H. G. LeDuc, "Quasi optical slot antenna SIS mixer," *IEEE Trans. Microwave Theory Tech.,* vol. 40, no. 9, 1992.

[13] R. L. Rogers and D. P. Neikirk, "Use of broadside twin element antennas to increase efficiency on electrically thick dielectric substrates," *Int. J. of IR and MM Waves,* vol. 10, pp. 697–728, 1988.

[14] D. Kasilingam and D. B. Rutledge, "Focusing properties of small lenses," *Int. J. of IR and MM Waves,* vol. 7, no. 10, pp. 1631–1647, 1986.

[15] M. Born and E. Wolf, *Principles of Optics,* New York: Pergamon, 2nd ed., 1964.

[16] M. J. Wengler, D. P. Woody, R. E. Miller, and T. G. Phillips, "A low noise receiver for millimeter and submillimeter wavelength," *Int. J. of IR and MM Waves,* vol. 6, pp. 697–706, 1985.

[17] T. H. Büttgenbach, R. E. Miller, M. J. Wengler, D. M. Watson, T. G. Phillips, "A broad-band low-noise SIS receiver for submillimeter astronomy," *IEEE Trans. Microwave Theory Tech.,* vol. 36, no. 12, pp. 1720–1726, 1988.

[18] C. Zah, D. Kasilingam, J. S. Smith, D. B. Rutledge, T.-C. Wang and S. E. Schwarz, "Millimeter wave monolithic Schottky diode imaging arrays," *Int. J. of IR and MM Waves,* vol. 6, no. 10, pp. 981–997, 1985.

[19] A. Skalare, Th. de Graauw, and H. van de Stadt, "A planar dipole array antenna with an elliptical lens," *Microwave and Optical Tech. Lett.,* vol. 4, no. 1, 1991.

[20] C. J. Alder, C. R. Brewitt-Taylor, M. Dixon, R. D. Hodges, L. D. Irving, H. D. Rees, "Microwave and millimeter-wave receivers with integral antenna," *IEEE Proc.-H,* vol. 138, 1991.

[21] D. F. Filipovic, S. S. Gearhart, and G. M. Rebeiz, "Double slot antennas on hyperhemispherical, elliptical, and extended hemispherical dielectric lenses," *IEEE Microwave Theory Tech.,* this issue.

[22] D. P. Neikirk, W. W. Lam, D. B. Rutledge, "Far-infrared microbolometer detectors," *Int. J. of IR and MM Waves,* vol. 5, pp. 245–276, 1984.

[23] Radiometer Physics, Bergwiesenstr. 15, Meckenheim, FRG.

[24] J. Ruze, "Antenna tolerance theory—A review," *Proc. IEEE,* vol. 54, no. 4, pp. 633, 1966.

[25] H. T. Friis, "A note on a simple transmission formula," *Proc. IRE,* vol. 34, pp. 254–256, 1946.

[26] W. C. Jakes, *Antenna Engineering Handbook,* H. Jasik, Ed., New York: McGraw-Hill, ch. 10, 1961.

[27] B. K. Kormanyos, C. C. Ling, and G. M. Rebeiz, "A planar wideband millimeter-wave subharmonic receiver," in *IEEE MTT-S Int. Microwave Symp. Dig.,* 1991, pp. 213–216.

[28] T. H. Büttgenbach, J. B. Keene, C. K. Walker, and T. G. Phillips, "Submillimeter detection of extragalactic C_I emission: IC342," *Astrophysical Journal Letters,* vol. 397, pp. L15–L17, 1992.

[29] T. H. Büttgenbach, J. B. Keene, T. G. Phillips, and R. E. Miller, "The small scale structure of C_I in Orion," in preparation, 1993.

[30] T. H. Büttgenbach, H. G. LeDuc, P. D. Maker, and T. G. Phillips, "A fixed tuned broadband matching structure for submillimeter SIS receivers," *IEEE Trans. Applied Supercond.,* vol. 2, no. 2, Sept. 1992.

[31] C. K. Walker, J. W. Kooi, M. Chan, H. G. LeDuc, J. E. Carlstrom, and T. G. Phillips, "A low-noise 492 GHz SIS waveguide receiver," *Int. J. of IR and MM Waves,* vol. 13, no. 6, pp. 785, 1992.

[32] T. H. Büttgenbach and T. L. Rose, "Planar antenna structures for SIS receivers," in preparation.

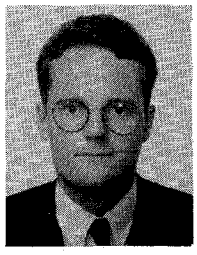

Thomas H. Büttgenbach (S'91) was born in Bergisch Gladbach, Federal Republic of Germany, on June 10, 1962. He received his Vordiplom from the University of Cologne in 1985 and was elected to be a member of the *Studienstiftung des Deutschen Volkes*. From 1986 to 1987 he was a Fulbright fellow at the California Institute of Technology, Pasadena, where, in 1987, he entered the Ph.D. program in physics.

In 1989 he received the award *zur Förderung selbständiger junger Menschen* from the German Foundation for Science. For the 1989/1990 academic year he received a fellowship from the Schlumberger foundation and in 1991 he was awarded the Stemple Memorial Price for outstanding progress in research in physics at Caltech. His research is in the field of quasi-optical techniques for superconducting receivers in the millimeter and submillimeter wavelengths bands and radio astronomical observations of interstellar clouds in those bands.

Mr. Büttgenbach is a member of the American Physical Society.